Supporting Information

Chan et al. 10.1073/pnas.1205459109

SI Materials and Methods

Generation of 293T Cells Stably Expressing Heat Shock Protein 90 Isoform α/β/p23 Split Renilla Luciferase Reporter and EGFP-Firefly Luciferase Fusion Reporter. To monitor the effect of different heat shock protein 90 (Hsp90) inhibitors on cell proliferation, we used a second imaging reporter expressing Firefly luciferase (FL) and EGFP (EGFP-FL) under the control of an ubiquitin-C promoter (1). The effects of different inhibitors on Hsp90(α/β)/p23 interactions were monitored by Renilla luciferase (RL) imaging, and their effects on cell proliferation were monitored by FL imaging because their respective substrates (coelenterazine and D-luciferin) do not cross-react (2). This EGFP-FL reporter was introduced into 293T cells stably expressing Hsp90α/p23 or Hsp90β/p23 split RL reporters via lentiviral transduction as reported previously (1). Single-cell colonies were selected by plating cells at low densities (1,000–3,000 cells per 10-cm^2 dish) and FL imaging (1 min using a cooled CCD camera) upon addition of D-luciferin in PBS (0.225 mg/mL final concentration).

Screening of Structural Analogs of Lead Compound CP9. To identify more potent structural analogs of CP9, 293T cells stably expressing Hsp90(α/β)/p23 split RL reporters and FL-EGFP fusion reporters were treated with 62 different CP9 analogs (Asinex) at 10 μM for 24 h in duplicate wells. CP9 (0.3–10 μM), 17-AAG (10 μM), and PU-H71 (5 μM) were used as positive controls in triplicate wells in 96 black-walled plates. The efficacy of the analogs in disrupting Hsp90(α/β)/p23 interactions and cell proliferation was monitored by RL imaging (2 h after the addition of EnduRen at 30 μM final concentration) followed by FL imaging (10 min after the addition of D-luciferin at 0.225 mg/mL final concentration) using a cooled CCD camera (1 min and 10 s for RL and FL imaging, respectively). RL signals were normalized to FL signals to account for the effect of the analogs on cell proliferation. Dose–response curves (six twofold serial dilutions) for the disruption of Hsp90 (α/β)/p23 interactions in the stable cells also were generated for the top eight compounds (A17, A15, A29, A31, A39, A58, A61, and A65) and were compared with that of CP9. The effect of the CP9 analogs on the degradation of Hsp90 client proteins in 293T cells also was monitored by Western blotting as described in the main text. The IC_{50} of the lead compound, A17, was determined by alamarBlue Assay.

Effect of CP9 on Proliferation of Doxorubicin-Resistant Lung Cancer Cells. To determine the effect of CP9 on proliferation of doxorubicin (DOX)-resistant V79/ADR cells, 3×10^4 V79 and V79/ADR cells were plated in each well of a 96-well plate and allowed to attach for 24 h. Cells were treated with 0.31–10 μM DOX in the presence of 8 μM CP9 or PU-H71 or carrier (control) for 24 h. Cell proliferation was assayed by alamarBlue Assay as described in the main text.

1. Lois C, Hong EJ, Pease S, Brown EJ, Baltimore D (2002) Germline transmission and tissue-specific expression of transgenes delivered by lentiviral vectors. *Science* 295:868–872.

2. Bhaumik S, Gambhir SS (2002) Optical imaging of Renilla luciferase reporter gene expression in living mice. *Proc Natl Acad Sci USA* 99:377–382.

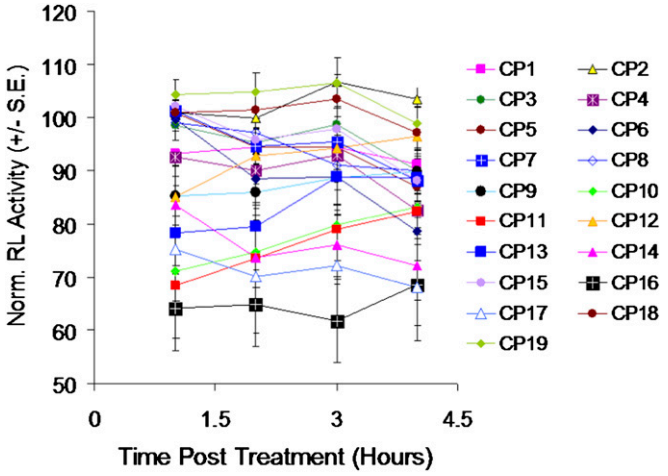

Fig. S1. Elimination of nonspecific RL Inhibitors from HTS. Quantitation of bioluminescence signals from Fig. 2*A*. The radiance for the quadruplicate wells was averaged and normalized to that of carrier control-treated cells. Results are expressed as mean ± SEM. Compounds that nonspecifically inhibit RL activities (>20% vs. carrier control-treated cells) were eliminated.

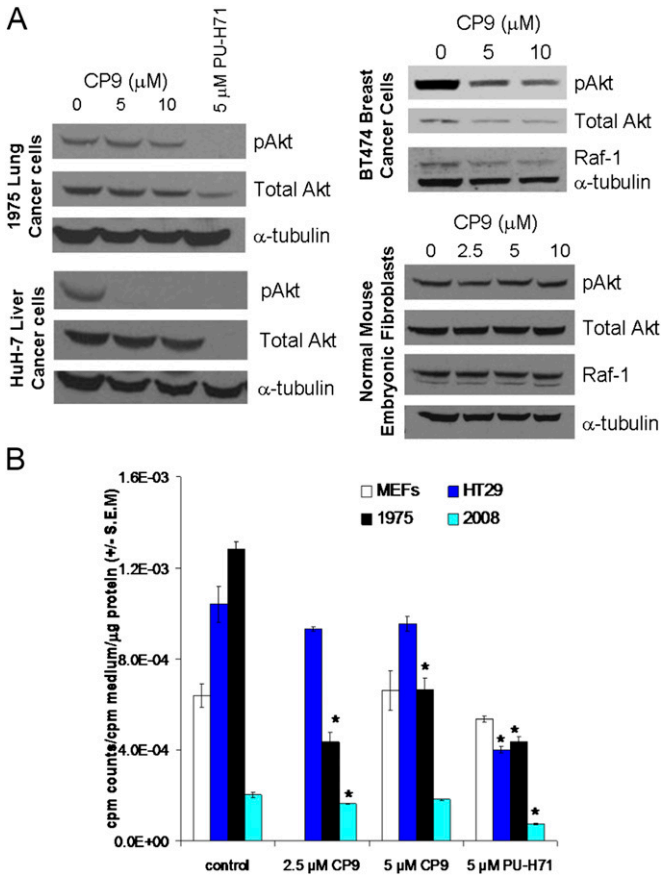

Fig. S2. Degradation of multiple Hsp90 client proteins by CP9 in different cancer cell lines. (*A*) The effect of CP9 on expression of Raf-1, phosphorylated Akt (pAkt), and total Akt in 1975 (lung cancer), BT474 (breast cancer), and HuH-7 (liver cancer) cells and in normal mouse embryonic fibroblasts (MEFs) was determined by Western blotting as Fig. 3*A*. α-Tubulin was used a loading control. (*B*) The effect of CP9 on mammalian thymidine kinase activity in 1975, 2008, and HT29 cells and in MEFs was determined by [^{3}H]3-fluorodeoxy-thymidine cell-uptake studies 48 h after treatment as described in Fig. 4*B*. Results are expressed as mean counts·min^{-1}·microgram protein^{-1}·initial dose^{-1} ± SEM. *$P < 0.05$ vs. carrier control-treated cells.

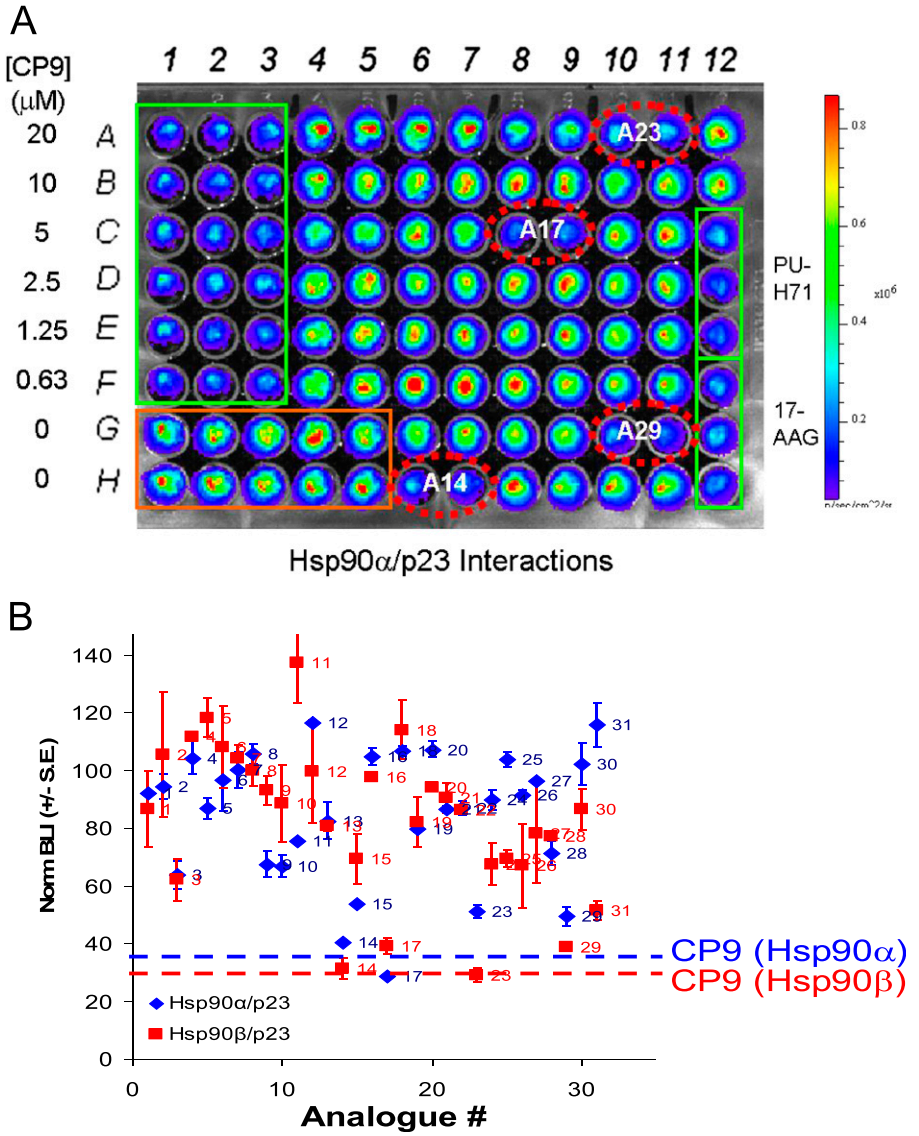

Fig. S3. Evaluation of the efficacy of CP9 analogs in disrupting Hsp90(α/β)/p23 interactions in 293T cells. To evaluate the efficacy of compounds that are structurally similar to CP9, 293T-FG cells stably expressing Hsp90(α/β)/p23 split RL reporters and EGFP-FL fusion reporter were treated with of CP9 (0.63–10 μM) and its 62 different analogs (10 μM) or carrier controls for 24 h. Duplicate wells were used for each analog. Bioluminescence imaging (BLI) of the effects of CP9 and its analogs on Hsp90(α/β)/p23 interactions (complemented RL activities) was performed as in Fig. 1*B*. Hsp90(α/β)/p23 interactions were monitored by RL imaging, and cell proliferation was determined by FL imaging. (*A*) RL imaging of the inhibition of Hps90α/p23 interactions by CP9 and 31 of its 62 analogs. A six-point dose–response curve was established for CP9 (rows A–F, columns 1–3). Duplicate wells were used for each analog concentration. PU-H71 and 17-AAG were used as positive controls at 10 μM in triplicate (rows C–F/column 12). Cells treated with 1% DMSO served as carrier control-treated (rows G and H, columns 1–5). Results from the 31 analogs are shown here. Some of the lead compounds (A14, A17, A23, and A29) are marked by dotted red circles. (*B*) CP9 and its analogs led to different levels of inhibition of Hsp90(α/β)/p23 interactions. To account of the effect of CP9 and its analogs on the inhibition cell proliferation, RL signals were normalized to FL signals, followed by normalization to signals of carrier control-treated cells; results are shown as mean ± SEM. The numbers next to each diamond (Hsp90α/p23) and square (Hsp90β/p23) denote the analog number (A1–A31). Dotted lines denote the level of inhibition of Hsp90(α/β)/p23 interactions by the parent compound CP9 at 10 μM.

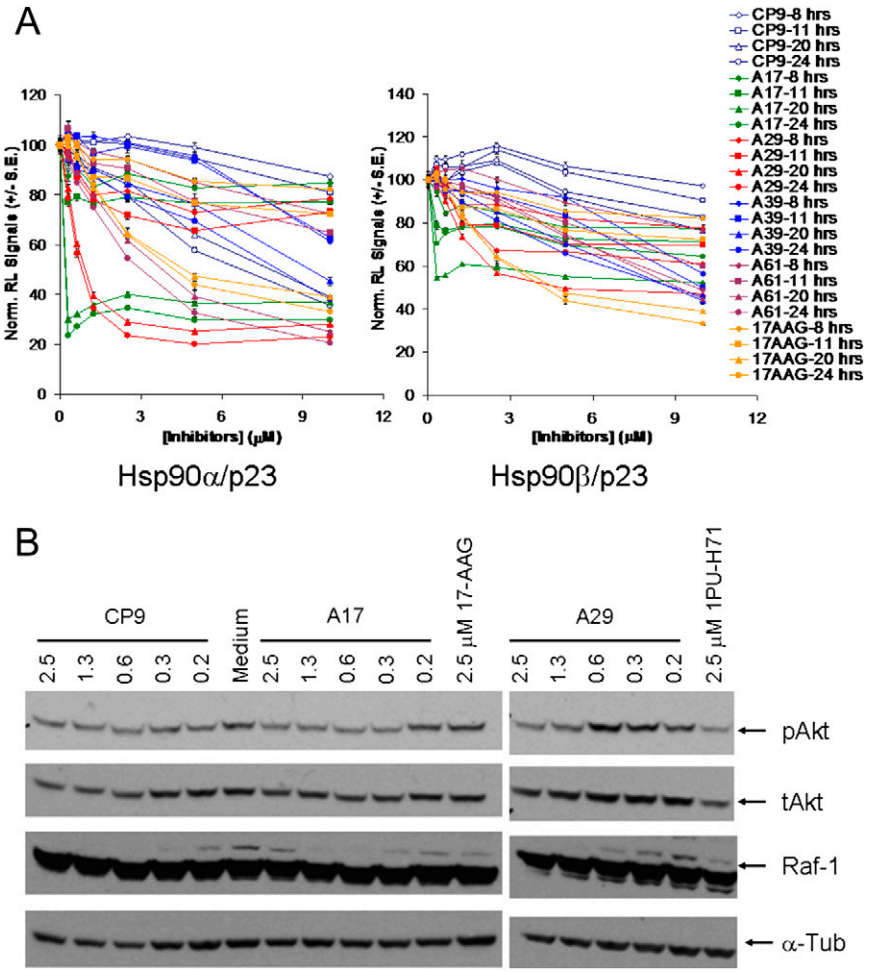

Fig. S4. Characterization of lead CP9 analogs. (*A*) Time- and dose-dependent decrease in RL signals in 293Tα-FG and 293Tβ-FG cells by CP9 and its four most potent analogs. Cells stably expressing the Hsp90(α/β)/p23 split RL reporters and EGFP-FL fusion proteins were treated with indicated concentrations of CP9, its analogs, or carrier controls before BLI of RL signals upon addition of EnduRen. RL signals at each drug concentration and at each time point were normalized to that of carrier control-treated cells and expressed as mean ± SEM. (*B*) Dose-dependent decreases in Hsp90 client proteins Raf-1, pAkt, and total Akt in 293Tα/p23-FG cells by CP9 and its analogs A17 and A29 were determined by Western blotting as in Fig. 3*A*. Cells treated with PU-H71 and 17-AAG (2.5 μM) served as positive controls. α-Tubulin was used a loading control.

Table S1. Chemical structures of the top 19 lead compounds (CP1–19) from the HTS of Hsp90 inhibitors

Table S1

The structure of the known Hsp90 inhibitor PU-H71 is shown also.

Table S2. Structural analogs of the lead compound CP9

Table S2

The compounds CP9 and A1-A62 that belong to the class of [2-(trifluoromethyl)pyrimidin-2-yl)thio)acetamides were selected rationally for structural activity relationship (SAR) studies.